Research Article Vol. 6, No. 4 / April 2019 / Optica 442

Quasi-phase-matched high-harmonic generation in gas-filled hollow-core photonic crystal fiber

Florian Wiegandt,[1,*] Patrick N. Anderson,[1] Fei Yu,[2,3] Daniel J. Treacher,[1] David T. Lloyd,[1] Peter J. Mosley,[2] Simon M. Hooker,[1] and Ian A. Walmsley[1]

[1]Clarendon Laboratory, Department of Physics, University of Oxford, OX1 3PU, UK
[2]Centre for Photonics and Photonic Materials, Department of Physics, University of Bath, Bath, UK
[3]Current address: R&D Center of High Power Laser Components, Shanghai Institute of Optics and Fine Mechanics, Chinese Academy of Sciences, Shanghai 201800, China
*Corresponding author: florian.wiegandt@physics.ox.ac.uk

Received 15 October 2018; revised 28 February 2019; accepted 6 March 2019 (Doc. ID 348189); published 4 April 2019

High-order harmonic generation (HHG) provides a promising tabletop source of coherent short wavelength radiation. However, the low generation efficiency limits the mean photon flux of HHG sources when driven with low average power, kHz repetition rate lasers. The HHG flux could be increased by employing MHz repetition rate driving lasers. However, the low pulse energy necessitates tight focusing, which limits the effective interaction volume. Generating harmonics in a gas-filled photonic crystal fiber (PCF) mitigates this problem, but for both free focus and PCF targets, the HHG conversion efficiency is optimized at technologically challenging multibar gas pressures. Here, we perform HHG with μJ-level driving pulses in a hollow-core PCF. We observe dramatic 60-fold enhancement of the HHG flux through a time-multiplexed multimodal quasi-phase-matching technique at low gas pressures. We also observe high harmonic photon energies up to 61.6 eV with continuous spectral tunability made possible by controlled ionization-induced blue shifting of the driving laser.

https://doi.org/10.1364/OPTICA.6.000442

1. INTRODUCTION

Compact, bright sources of coherent extreme ultraviolet (XUV) radiation open new opportunities for applications that require a high average photon flux such as lithography and coherent imaging. One approach to generate such light sources is high harmonic generation (HHG) [1,2], in which femtosecond-duration laser pulses from high repetition rate, high average power near-infrared (NIR) lasers are focused into a noble gas. Efficient operation of HHG sources demands a sufficiently high peak intensity. When using mJ-level NIR driving pulses at low repetition rates, conversion efficiencies of 10^{-6}–10^{-5} have been reached [3–5], corresponding to a XUV photon flux per harmonic of $\sim 10^9$ photons s^{-1}. When using high pulse repetition rate laser systems, pulse post-compression and stronger focusing of the driving pulses is necessary due to the comparatively low pulse energy (in the range of tens of microjoules) currently deliverable from ultrafast, high average power laser systems such as thin disk [6], fiber lasers [7] or optical parametric chirped-pulse amplifiers (OPCPA) [8]. As a result of tight focusing, the interaction volume is greatly reduced [9]. Studies have shown that in the tight-focus regime the HHG absorption limit can be reached [10,11], but elaborate target geometries and high pumping speeds are required to maintain high vacuum elsewhere in the beamline. In cases where the density required for absorption-limited generation cannot be reached, the HHG efficiency can drop below 10^{-10} [12].

These limitations can be mitigated by coupling the laser into a gas-filled hollow core optical waveguide with a small core diameter d in which the light propagates in confined waveguide eigenmodes [13]. However, the transmission loss of the driving laser at wavelength λ_0 in conventional capillary waveguides scales as λ_0^2/d^3 and quickly becomes a limiting factor. Hollow-core PCF (HC-PCF) such as the Kagome type PCF or negative-curvature PCF (NC-PCF) [14] exhibit significantly lower guiding losses compared to a capillary with a similar d due to antiresonant guiding [15].

It has recently been demonstrated that nonlinear compression of pulses from a Ti:sapphire laser can be performed in a helium-filled Kagome PCF ($d = 46$ μm) yielding ~15 fs, ~50 μJ pulses that were subsequently used to generate high-order harmonics up to the 29th order (H29, $q = 29$) in an argon gas jet, placed directly behind the exit of the PCF [16]. HHG up to H13 of an 800 nm driving laser has also been demonstrated with 4.2 μJ, 30-fs pulses inside a Kagome PCF ($d = 15$ μm) in a proof-of-principle experiment [17] with a low conversion efficiency ($\sim 10^{-9}$) due to imperfect phase matching and the low coupling efficiency of the driver into the PCF.

Here, we report on HHG driven with μJ-level NIR pulses in NC-PCF at photon energies up to 61.6 eV. Further, we demonstrate that multimode quasi-phase-matching (MM-QPM) [18,19] of HHG in a NC-PCF leads to an order of magnitude enhancement of the HHG signal.

Efficient HHG in gases requires phase matching. In a gas-filled waveguide, the driving laser and the harmonic field propagate with different wave vectors k. Below a critical ionization level, the phase mismatch $\Delta k = k(\lambda_q) - qk(\lambda_0)$ can be minimized by adjusting the gas density [20]. However, due to the comparatively high waveguide dispersion in PCFs, phase-matching would require multi-atmosphere gas pressures resulting in strong XUV reabsorption and high gas loads onto the generation setup. An alternative approach is quasi-phase-matching (QPM) in which destructive interference of harmonic radiation emitted at different locations is inhibited by suppressing HHG periodically along the propagation axis. This can be achieved, for instance, through longitudinal intensity modulation of the driving laser with a period $L_{\mathrm{QPM}} = 2\pi j/|\Delta k|$, where j is the order of QPM. This allows for more efficient intensity buildup even when $\Delta k \neq 0$ at comparatively low gas pressures.

Several different schemes have been developed for on-axis amplitude modulation of the driving laser in an capillary waveguide [18,21,22]. In our experiment, it is realized by a variation of the MM-QPM scheme demonstrated in [3,18]. We achieve intensity modulation through beating of LP_{mn} waveguide modes [23] with different propagation constants β_{mn} and $\beta_{\mu\nu}$. The beating period is given by $L_B = 2\pi/|\beta_{mn} - \beta_{\mu\nu}| \approx 2\pi^2 d^2/|\lambda_0(u_{mn}^2 - u_{\mu\nu}^2)|$, where u_{mn} is the nth zero of the Bessel function of order $m-1$. Optimal MM-QPM is achieved if the gas density and pulse peak intensity are chosen such that $L_{\mathrm{QPM}} = L_B$.

In practice, exciting only two specific waveguide modes is difficult and the beating of a large number of modes results in complex longitudinal beating patterns [3,18]. To set more controllable experimental framework conditions for the test of MM-QPM in our NC-PCF, we developed an innovative concept to induce mode beating between pairs of waveguide modes: We use intermodal delay dispersion to temporally separate the modes excited by a pair of femtosecond pulses; this allows selected, isolated modes to be temporally overlapped at the exit of the NC-PCF. The concept of this intermodal delay-controlled QPM (IDC-QPM) is illustrated in Fig. 3(a) together with the results of a numerical unidirectional pulse propagation simulation [24] in Fig. 3(b), limited to the five lowest order LP_{0n} modes of the NC-PCF used in the experiment. A pair of identical NIR laser pulses, termed "control" and "drive," is generated in a Mach–Zehnder interferometer fitted with a variable delay stage in one interferometer arm. First, the control pulse is launched into a section of the NC-PCF exciting a set of LP modes. As the pulse propagates a distance z into the NC-PCF, modal dispersion causes the different modes to walk-off temporally. At the exit of the NC-PCF ($z = L$), the group delay between the fundamental mode LP_{01} and a given higher-order mode LP_{mn} can be expressed as $\tau_{mn} = L2\pi c/\lambda_0^2[(\partial^2\beta_{mn}/\partial\omega^2) - (\partial^2\beta_{01}/\partial\omega^2)]$, where c is the speed of light and ω is the angular frequency. We calculated the complex propagation constants of the core modes in our NC-PCF numerically by using commercial finite-element method software (*COMSOL*) following the approach reported in [25]. When the drive pulse is coupled into the fiber with a delay $\tau = \tau_{mn}$, the fundamental mode of the drive pulse overlaps with a higher-order mode of the control pulse close to the exit of the fiber. In the overlap region the carrier waves of both pulses interfere and cause amplitude modulation (AM) of the electric field, shown in the inset of Fig. 3(b).

A. Methods

In our experiment, we employ IDC-QPM to enhance the HHG conversion efficiency in a NC-PCF ($d = 22.5$ μm). This type of antiresonant guiding PCF, shown in Fig. 1(b), has a minimum attenuation of 0.06 dB/m at 690 nm with attenuation below 0.3 dB/m for wavelengths between 610 and 840 nm [26]. We drive HHG in argon and neon gas with 5–15 μJ, 30-fs (FWHM) pulses from a Ti:sapphire laser system operating at a pulse repetition rate of 1 kHz.

The experimental setup is shown in Fig. 1(a). Linear polarized laser pulses from a Ti:sapphire chirped-pulse amplifier (CPA) are attenuated to an energy of 5–15 μJ and spatially filtered. A pair of pulses is then generated in a Mach–Zehnder interferometer. The relative delay can be adjusted by changing the length of one interferometer arm, which can also be blocked to drive HHG with only a single laser pulse. The laser pulses are then coupled into a section of a NC-PCF ($L = 22.5$ mm) by means of an XYZ-translatable lens ($f = 75$ mm). We achieve a high coupling efficiency and NIR transmission of up to 90% through the NC-PCF section, which is mounted between two vacuum chambers. The first of these is filled with Ar or Ne gas at 800 mbar while high vacuum (10^{-5} mbar) is maintained throughout the second by using a 300 l/s turbomolecular pump.

To model the gas flow through the PCF we assume a turbulent, isothermal gas flow through the core that resembles the flow

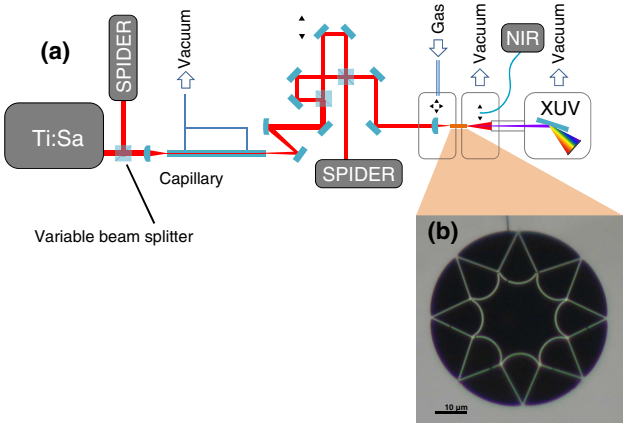

Fig. 1. Experimental setup. (a) A Ti:sapphire laser (KMLabs) delivers 1 mJ, 30 fs pulses at a repetition rate of 1 kHz and a central wavelength of 785 nm. The pulse duration is measured with spectral phase interferometry for direct electric field reconstruction (SPIDER). The pulse energy is reduced to 1–15 μJ by means of a variable beam splitter. After spatial filtering in an evacuated capillary, a pair of pulses is generated in a Mach–Zehnder interferometer fitted with a variable delay stage in one beam path. The pulses are then coupled into a section of a NC-PCF ($L = 22.5$ mm) using a lens mounted on a XYZ stage. The NC-PCF is filled with Ar or Ne gas at various pressures. The high-harmonic beam is analyzed in a flat-field XUV spectrometer (XUV) and the residual driving laser is analyzed in a fiber-coupled near-infrared spectrometer (NIR). (b) Microscope image of the NC-PCF used in the present experiment. The diameter of the hollow core (shortest distance between two opposite hypocycloids) is 22.5 μm.

of a compressible gas through a cylindrical pipe with diameter d and length L [27]. In this regime the different gas pressures at the entrance and exit of the NC-PCF, P_0 and P_L, lead to a longitudinal pressure profile along the spatial coordinate z, which can be approximated as $P(z) \approx [P_0 + (z/L)(P_L^2 - P_0^2)]^{1/2}$. This pressure gradient causes the coherence length to vary continuously along the fiber. Furthermore, the strength of the XUV emission along z depends on the number of XUV emitters present at the position z, whereas the reabsorption of the radiation obeys Beer–Lambert's law and decreases with decreasing gas density. Since a high entrance pressure $P_0 = 0.8$ bar is used in the present experiment, the absorption length is less than 100 μm throughout 95% of the fiber length [28]. Hence, most of the observed XUV radiation is generated close to the exit of the NC-PCF. The XUV output of the NC-PCF is analyzed using a flat field XUV spectrometer and the average photon flux is measured with a XUV photodiode mounted behind a 400 nm thick Al-filter to block the residual driving laser. Additionally, a fiber-coupled NIR spectrometer is used to characterize the residual driving laser.

2. RESULTS AND DISCUSSION

A. Non-Phase-Matched HHG in a NC-PCF

Using an argon gas fill we observe harmonics between H19 and H23 when single, 30 fs, 5 μJ drive pulses are launched into the NC-PCF. For neon gas, the threshold pulse energy at which we observe the same harmonic orders lies at 10 μJ. Increasing the drive pulse energy to 15 μJ yields harmonics with energies up to 61.6 eV, as shown in Fig. 2(a). These are, to our knowledge, the highest photon energies reported to date for HHG in a NC-PCF. Figure 2(a) shows a typical wavelength comb with peaks located at high-order, odd-integer fractions of the fundamental driver wavelength, which is a clear signature of HHG [1]. The cutoff energy of 61.6 eV is in good agreement with the cutoff predicted by the semiclassical model of HHG [29] for a driver peak intensity of $\sim 2.3 \times 10^{14}$ W cm^{-2}.

The harmonic spectrum and the spectrum of the driving laser at the exit of the Ar-filled NC-PCF are shown in Figs. 2(b) and 2(c) for a range of pulse energies. For driver pulse energies above 7 μJ we observe spectral reshaping of the driving beam. It can be seen that the spectral reshaping of the driver depends on the incident pulse energy. This effect is caused by pulse self-compression and subsequent blue shift that has been discussed in the literature [30,31]. The magnitude of the blue shift is proportional to the ionization rate of the gas, and therefore larger at higher peak intensities [30]. As illustrated in Fig. 2(b), the blue shift of the driver translates onto the harmonic spectrum, yielding an XUV quasicontinuum at the highest input pulse energies. This behavior is known from previous theoretical studies and experiments reported in [16,32].

We note that no blue shift of the driver laser was observed when the NC-PCF was filled with neon gas. We measured an average spectral flux of approx. 1.14×10^6 photons s^{-1} nm^{-1} in H25 ($\sim 10^3$ photons per drive pulse) generated in Ne with 15 μJ pulses and an average flux of less than 5.9×10^5 photons s^{-1} nm^{-1} in H23 generated in Ar with 10 μJ pulses. The low conversion efficiency of $\sim 10^{-10}$ is mainly the result of poor phase matching.

B. Quasi-Phase-Matching

Intermodal delay-controlled QPM was achieved by coupling both driver and control pulses into the PCF with a specific relative delay. In Fig. 3(c) the integrated spectral intensity in a window spanning from H21 to H25 is shown as a function of delay τ between drive and control pulses, both attenuated to 5 μJ. At small relative delays $|\tau| < 50$ fs, the LP_{01} modes of the drive and control pulse overlap and the modulation in the brightness of H21–H25 resembles a high-order interferometric autocorrelation of drive and control pulse. The peaks located around the temporal overlap at $|\tau| > 50$ fs can be attributed to the temporal overlap of the LP_{01} mode of the driver pulse with the LP_{0n} and LP_{1n} ($n = 1,2,3$) modes of the control pulse close to the exit of the NC-PCF. In this work, since the drive and control pulses are identical, and both pulses are coupled into the same waveguide modes, the delay dependent variation of the harmonics intensity is symmetric around $\tau = 0$. For $\tau < 0$ the control pulse is coupled into the NC-PCF first while harmonics are generated when the drive pulse arrives. However, the situation is reversed for $\tau > 0$. Figure 3(c) shows, for a propagation distance of $z = 22.5$ mm,

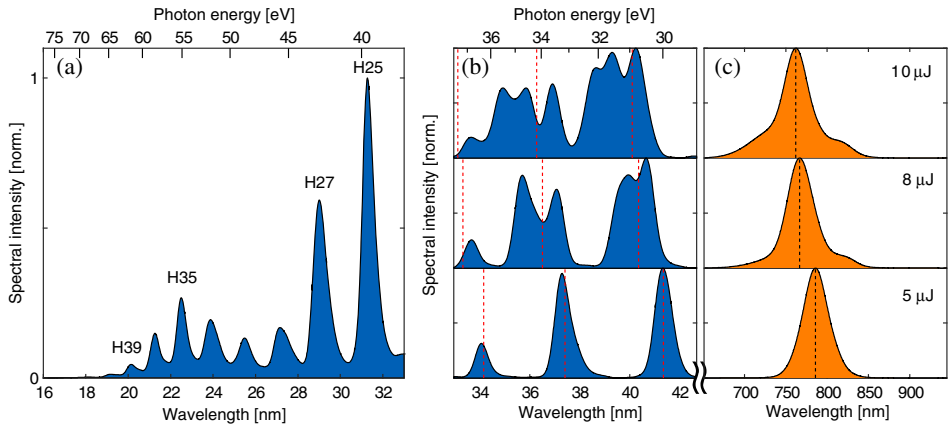

Fig. 2. Measured XUV and IR spectra. (a) Harmonic spectrum generated in Ne at an inlet pressure of 0.8 bar with single 15 μJ pulses. Harmonics up to H39 (20 nm, 61.6 eV) are detected. (b) Harmonic spectrum (H19–23) in Ar at a pressure of 0.1 bar and (c) spectrum of the driving laser measured at the exit of the NC-PCF for the same three pulse energies used in Fig. 2(b). The spectral broadening and blue shift of the driver due to nonlinear propagation in the NC-PCF is transferred to the harmonic spectrum. The red dashed lines indicate the central wavelength of the transmitted driving laser [Fig. 2(c), black lines] divided by the order q of different harmonics ($q = 19, 21, 23$).

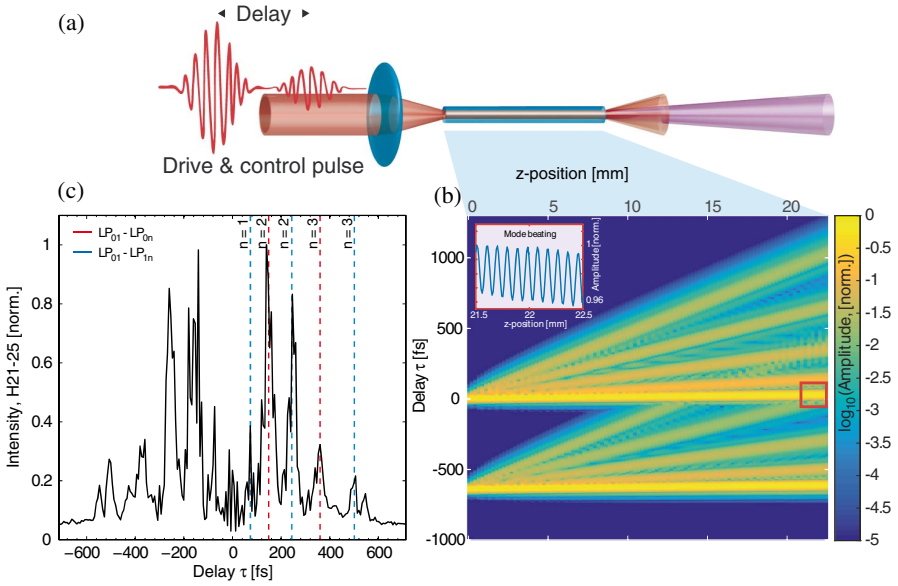

Fig. 3. Intermodal-delay-controlled QPM. (a) Concept and (b) simulation results of IDC-QPM for a set of five low-order waveguide modes (LP_{01} – LP_{05}). A control and a drive pulse are launched into a gas-filled section of a NC-PCF with a relative delay. Modal dispersion of the waveguide results in a temporal separation of higher-order spatial modes as the pulses propagate along the NC-PCF. Overlap of one higher-order mode of the control pulse with the fundamental mode of the drive pulse causes mode beating at the exit of the NC-PCF and rapid longitudinal modulation of the combined electric fields (inset). The amplitude modulation depth, 5% in the present case, is set by the relative intensity of the beating modes at the exit of the NC-PCF. (c) Experimental results: Intensity of H21-25 as a function of delay τ between drive and control pulse. The dashed lines indicate, for a propagation distance of $z = 22.5$ mm, the difference in group delay between various higher-order modes and the fundamental mode.

the group delays between various modes and the fundamental mode predicted by *COMSOL* calculations of the propagation constants and intermodal delays τ_{mn}. It is seen that the harmonic intensity shows clear maxima for $\tau = \tau_{mn}$, confirming our model of IDC-QPM. Figure 4(a) shows the harmonic spectrum (H21–H25) generated with pairs of 5 μJ pulses when the delay is precisely tuned to the enhancement peak at $\tau = 160$ fs in Fig. 3(c). Compared to the case when HHG is driven with single 10 μJ pulses (red curves), we observed a brightness enhancement of H21–25 by a factor of approximately 60.

In the present experiment a comparatively long section of NC-PCF was chosen to allow for a good temporal mode separation. To localize sufficient gas pressure for HHG at the exit of the NC-PCF, the front was held at 800 mbar, causing strong XUV reabsorption throughout almost the entire length of the NC-PCF. Hence, the benefits of using the PCF to purely extend the interaction length were limited.

To understand the effect of the density gradient in the NC-PCF we modelled the harmonic generation by MM-QPM in PCFs with uniform and nonuniform gas fills [33] (see Supplement 1). Figure 4(b) shows the modeled on-axis HHG yield as a function of input pressure. Our model shows that a uniformly filled NC-PCF would enable IDC-QPM at significantly lower input pressures while at the same time resulting in an additional order of magnitude enhancement (i.e., a 600-fold increase compared to the single pulse driver case) of the HHG yield.

In this proof-of-principle experiment no attempt was made to optimize the coupling of drive and control pulse into specific fiber modes (e.g., by using a spatial light modulator) [34]. Such modifications to the experiment have the potential to improve the overall HHG efficiency since all the available driving laser power could be preferentially coupled into fiber modes involved in MM-QPM. Furthermore, using drive and control pulse with orthogonal polarization could further improve the MM-QPM performance, as proposed in [19].

Even without these additional optimizations, with IDC-QPM we measured a flux of 10^8 photons per second per harmonic, averaged over H17–H23, corresponding to 10^5 photons per harmonic per laser shot and a conversion efficiency of launched NIR driving power into a single harmonic order of approx. 10^{-7}. This is about two orders of magnitude higher than the HHG conversion efficiency in HC-PCF reached in previous experiments [17].

Compared to HHG that is not phase matched and driven directly with few-microjoule pulses from 50 to 100 kHz Ti:sapphire lasers [9,35], the efficiency reached in the present experiment is approximately one order of magnitude higher and is comparable to the efficiency of HHG directly driven with a Yb-based fiber-laser system at a 100 kHz pulse repetition rates [10].

On the other hand, the conversion efficiency in the present experiment is one order of magnitude lower than quasi-phase-matched HHG in capillaries with mJ-level driving pulses [3] or phase-matched HHG in a tightly focused NIR beam [11]. In [11], it was shown that in a free-focused beam geometry the phase-matching pressure is inversely proportional to the square of the spot size; hence, a very high pumping speed is required to maintain a good vacuum in the experimental chamber. This can be a substantial experimental limitation. Phase-matching HHG in a focused NIR beam with a size similar to the mode field diameter of the NC-PCF used in our experiment would require pumping speeds well exceeding 10^3 l/s to maintain a vacuum below 10^{-2} mbar in the target chamber [11].

The harmonic fluxes generated using the driving pulse energy and peak power in the present experiment opens the prospect

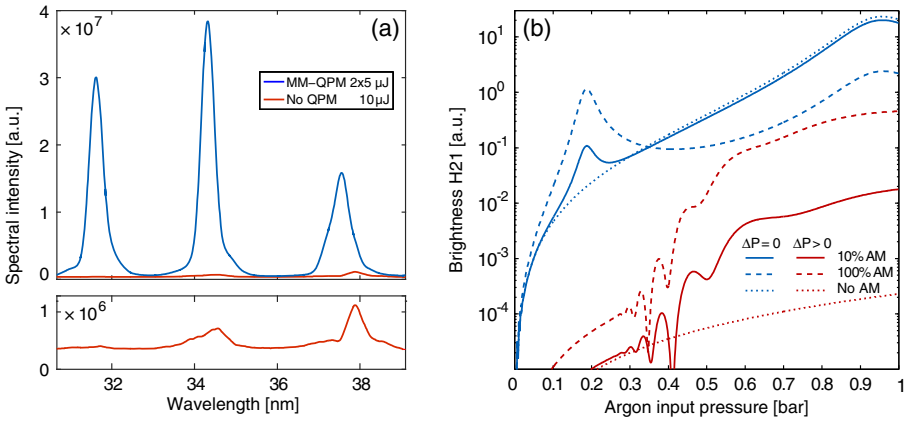

Fig. 4. Enhancement of the HHG flux due to MM-QPM. (a) Experimental harmonic spectrum H21–25 driven with pairs of 5 μJ pulses (delay $\tau = 190$ fs) with IDC-QPM (blue curve) and driven with single 10 μJ pulses without any QPM (red curves); the bottom panel shows the same single-pulse data but rescaled. The brightness enhancement of H21–25 by a factor of ∼60 is the result of IDC-QPM. (b) Modeled on-axis yield of H21 in the NC-PCF used in the present experiment for beating of the LP_{01} with LP_{13} mode in case of a uniform argon pressure in the NC-PCF, $\Delta P = (P_0 - P_L) = 0$, (all blue lines) and in case of a longitudinal pressure profile, $\Delta P > 0$ (all red lines). In both cases, the largest brightness enhancement is expected for beating of the LP_{01} with LP_{13} mode assuming 100% amplitude modulation (AM) in case of equally intense modes (dashed lines) and 10% AM in case of a weak LP_{13} mode (solid lines). Compared to the case where a pressure gradient is present in the NC-PCF, as in the present experiment, the model suggests further enhancement due to IDC-QPM at a uniform filling pressure of ∼200 mbar (solid & dashed blue lines). The dotted lines correspond to the case when drive and control pulse propagate in the same mode without mode beating. The blue dotted line indicates full phase matching at a uniform pressure close to 1 bar. Even though, the HHG conversion efficiency is highest at this pressure, the resulting high gas load is experimentally challenging.

of scaling efficient HHG to few-MHz repetition rates and high average driving powers using Yb-based thin-disk lasers, fiber CPAs, or high repetition rate, optical parametric chirped-pulse amplifiers (OPCPA) [7,8,36,37]. OPCPAs can deliver high peak power pulses in the mid-infrared (MIR). However, HHG with MIR pulses is more of a challenge since the phase-matching pressure scales with λ^2 [38]. Therefore, quasi-phase-matching techniques of the type described here could be of even greater importance for long wavelength driving laser pulses.

Driving HHG in the NIR with lanthanide-based fiber CPAs and thin-disk lasers requires pulse compression. Pulse post-compression has recently been demonstrated in gas-filled NC-PCFs [39,40] and Kagome PCFs [16] and has enabled wavelength-tunable HHG in a gas jet placed directly behind the output of the fiber. By generating directly in a NC-PCF and employing IDC-QPM, we reach at least 10 times higher conversion efficiency.

We note that we did not observe any significant damage to the NC-PCF over an operation period of several hours, even at average driving power beyond 15 mW. We also note that continuous power of up to 36 W has been guided within a NC-PCF with a similar design [41]. Hence, scaling our approach to multiwatt NIR or MIR average driving powers provides a promising route to high average power, short wavelength light sources extending into the soft x-ray region.

3. CONCLUSION

In conclusion, we have demonstrated HHG with few-μJ laser pulses in a Ne-filled NC-PCF up to what we believe are unprecedented high photon energies approaching the aluminum L-edge (72.8 eV). For Ar-filled NC-PCFs, we found that a gas ionization-induced and pulse peak power dependent blue shift of the driving laser was translated to the HHG spectrum and enables wavelength-tunable XUV generation directly in the NC-PCF. We also demonstrated what we believe is a new scheme to control MM-QPM in a NC-PCF through intermodal delay dispersion (IDC-QPM). We showed that IDC-QPM can increase the XUV flux by almost two orders of magnitude, leading to photon flux of 10^5 photons per harmonic order per laser shot. Further optimization of our approach and increasing the pulse repetition rate to the hundred kHz or even multi-MHz domain could increase the average XUV flux beyond 10^{12} photons s^{-1}, enabling many applications that require a compact, bright source of coherent XUV radiation.

Funding. Engineering and Physical Sciences Research Council (EPSRC) (EP/L015137/1); H2020 Marie Skłodowska-Curie Actions (MSCA) (641272).

See Supplement 1 for supporting content.

REFERENCES

1. A. L'Huillier, K. J. Schafer, and K. C. Kulander, "Higher-order harmonic generation in xenon at 1064 nm: The role of phase matching," Phys. Rev. Lett. **66**, 2200–2203 (1991).
2. P. B. Corkum, "Plasma perspective on strong field multiphoton ionization," Phys. Rev. Lett. **71**, 1994–1997 (1994).
3. M. Zepf, B. Dromey, M. Landreman, P. Foster, and S. M. Hooker, "Bright quasi-phase-matched soft-X-ray harmonic radiation from argon ions," Phys. Rev. Lett. **99**, 143901 (2007).
4. E. Constant, D. Garzella, P. Breger, E. Mével, C. Dorrer, C. L. Blanc, F. Salin, and P. Agostini, "Optimizing high harmonic generation in absorbing gases: model and experiment," Phys. Rev. Lett. **82**, 1668–1671 (1999).
5. P. Rudawski, C. M. Heyl, F. Brizuela, J. Schwenke, A. Persson, E. Mansten, R. Rakowski, L. Rading, F. Campi, B. Kim, P. Johnsson, and A. L'Huillier, "A high-flux high-order harmonic source," Rev. Sci. Instrum. **84**, 073103 (2013).
6. J. Brons, V. Pervak, D. Bauer, D. Sutter, O. Pronin, and F. Krausz, "Powerful 100-fs-scale Kerr-lens mode-locked thin-disk oscillator," Opt. Lett. **41**, 3567–3570 (2016).

7. C. Gaida, M. Gebhardt, F. Stutzki, C. Jauregui, J. Limpert, and A. Tünnermann, "Thulium-doped fiber chirped-pulse amplification system with 2 GW of peak power," Opt. Lett. **41**, 4130–4133 (2016).
8. N. Thiré, R. Maksimenka, B. Kiss, C. Ferchaud, P. Bizouard, E. Cormier, K. Osvay, and N. Forget, "4-W, 100-kHz, few-cycle mid-infrared source with sub-100-mrad carrier-envelope phase noise," Opt. Express **25**, 1505–1514 (2017).
9. F. Lindner, W. Stremme, M. G. Schatzel, F. Grasbon, G. G. Paulus, H. Walther, R. Hartmann, and L. Struder, "High-order harmonic generation at a repetition rate of 100 kHz," Phys. Rev. A **68**, 013814 (2003).
10. A. Cabasse, G. Machinet, A. Dubrouil, E. Cormier, and E. Constant, "Optimization and phase matching of harmonic generation at high repetition rate," Opt. Lett. **37**, 4618–4620 (2012).
11. J. Rothhardt, M. Krebs, S. Hädrich, S. Demmler, J. Limpert, and A. Tünnermann, "Absorption-limited and phase-matched high harmonic generation in the tight focusing regime," New J. Phys. **16**, 033022 (2014).
12. A. Vernaleken, J. Weitenberg, T. Sartorius, P. Russbueldt, W. Schneider, S. L. Stebbings, M. F. Kling, P. Hommelhoff, H.-D. Hoffmann, R. Poprawe, F. Krausz, T. W. Hänsch, and T. Udem, "Single-pass high-harmonic generation at 20.8 MHz repetition rate," Opt. Lett. **36**, 3428–3430 (2011).
13. E. A. J. Marcatili and R. A. Schmeltzer, "Hollow metallic and dielectric waveguides for long distance optical transmission and lasers," Bell Syst. Tech. J. **43**, 1783–1809 (1964).
14. F. Yu and J. C. Knight, "Negative curvature hollow-core optical fiber," IEEE J. Sel. Top. Quantum Electron. **22**, 4400610 (2016).
15. M. A. Duguay, Y. Kokubun, T. L. Koch, and L. Pfeiffer, "Antiresonant reflecting optical waveguides in SiO2-Si multilayer structures," Appl. Phys. Lett. **49**, 13–15 (1986).
16. F. Tani, M. H. Frosz, J. C. Travers, and P. S. J. Russell, "Continuously wavelength-tunable high harmonic generation via soliton dynamics," Opt. Lett. **42**, 1768–1771 (2017).
17. O. Heckl, C. Baer, C. Kränkel, S. Marchese, F. Schapper, M. Holler, T. Südmeyer, J. Robinson, J. Tisch, F. Couny, P. Light, F. Benabid, and U. Keller, "High harmonic generation in a gas-filled hollow-core photonic crystal fiber," Appl. Phys. B **97**, 369–373 (2009).
18. B. Dromey, M. Zepf, M. Landreman, and S. M. Hooker, "Quasi-phase-matching of harmonic generation via multimode beating in waveguides," Opt. Express **15**, 7894–7900 (2007).
19. L. Liu, Z. Lewis, K. O'Keeffe, and S. M. Hooker, "Quasi-phase-matching of high-order-harmonic generation using multimode polarization beating," Phys. Rev. A **87**, 023810 (2013).
20. C. G. Durfee III, A. R. Rundquist, S. Backus, C. Herne, M. M. Murnane, and H. C. Kapteyn, "Phase matching of high-order harmonics in hollow waveguides," Phys. Rev. Lett. **83**, 2187–2190 (1999).
21. H. Ren, A. Nazarkin, J. Nold, and P. S. Russell, "Quasi-phase-matched high harmonic generation in hollow core photonic crystal fibers," Opt. Express **16**, 17052–17059 (2008).
22. E. A. Gibson, A. Paul, N. Wagner, R. Tobey, D. Gaudiosi, S. Backus, I. P. Christov, A. Aquila, E. M. Gullikson, D. T. Attwood, M. M. Murnane, and H. C. Kapteyn, "Coherent soft X-ray generation in the water window with quasi-phase matching," Science **302**, 95–98 (2003).
23. T. Pfeifer and M. C. Downer, "Direct experimental observation of periodic intensity modulation along a straight hollow-core optical waveguide," J. Opt. Soc. Am. B **24**, 1025–1029 (2007).
24. M. Kolesik, J. Moloney, and M. Mlejnek, "Unidirectional optical pulse propagation equation," Phys. Rev. Lett. **89**, 283902 (2002).
25. F. Yu and J. C. Knight, "Spectral attenuation limits of silica hollow core negative curvature fiber," Opt. Express **21**, 21467–21471 (2013).
26. F. Yu, "Hollow core negative curvature optical fibres," Ph.D. thesis (University of Bath, 2013), p. 100.
27. W. Wissdorf, D. Müller, Y. Brachthäuser, M. Langner, V. Derpmann, S. Klopotowski, C. Polaczek, H. Kersten, K. Brockmann, and T. Benter, "Gas flow dynamics in inlet capillaries: evidence for non laminar conditions," J. Am. Soc. Mass Spectrom. **27**, 1550–1563 (2016).
28. CXRO, 2010, www.cxro.lbl.gov.
29. A. L'Huillier, M. Lewenstein, P. Salieres, and P. Balcou, "High-order harmonic-generation cutoff," Phys. Rev. A **48**, R3433 (1993).
30. S. C. Rae and K. Burnett, "Detailed simulations of plasma-induced spectral blueshifting," Phys. Rev. A **46**, 1084–1090 (1992).
31. M. F. Saleh, W. Chang, P. Hölzer, A. Nazarkin, J. C. Travers, N. Y. Joly, P. S. Russell, and F. Biancalana, "Theory of photoionization-induced blueshift of ultrashort solitons in gas-filled hollow-core photonic crystal fibers," Phys. Rev. Lett. **107**, 203902 (2011).
32. S. C. Rae and K. Burnett, "Generation and propagation of high-order harmonics in a rapidly ionizing medium," Phys. Rev. A **50**, 3438–3446 (1994).
33. C. M. Heyl, C. L. Arnold, A. Couairon, and A. L'Huillier, "Introduction to macroscopic power scaling principles for high-order harmonic generation," J. Phys. B **50**, 013001 (2017).
34. D. Walter, T. Pfeifer, C. Winterfeldt, R. Kemmer, R. Spitzenpfeil, G. Gerber, and C. Spielmann, "Adaptive spatial control of fiber modes and their excitation for high-harmonic generation," Opt. Express **14**, 3433–3442 (2006).
35. C. M. Heyl, J. Güdde, A. L'Huillier, and U. Höfer, "High-order harmonic generation with μJ laser pulses at high repetition rates," J. Phys. B **45**, 074020 (2012).
36. C. J. Saraceno, F. Emaury, O. H. Heckl, C. R. E. Baer, M. Hoffmann, C. Schriber, M. Golling, T. Südmeyer, and U. Keller, "275 W average output power from a femtosecond thin disk oscillator operated in a vacuum environment," Opt. Express **20**, 23535–23541 (2012).
37. F. Emaury, A. Diebold, C. J. Saraceno, and U. Keller, "Compact extreme ultraviolet source at megahertz pulse repetition rate with a low-noise ultrafast thin-disk laser oscillator," Optica **2**, 980–984 (2015).
38. A. D. Shiner, C. Trallero-Herrero, N. Kajumba, H.-C. Bandulet, D. Comtois, F. Legare, M. Giguere, J.-C. Kieffer, P. B. Corkum, and D. M. Villeneuve, "Wavelength scaling of high harmonic generation efficiency," Phys. Rev. Lett. **103**, 073902 (2009).
39. F. Köttig, F. Tani, C. M. Biersach, J. C. Travers, and P. S. Russell, "Generation of microjoule pulses in the deep ultraviolet at megahertz repetition rates," Optica **4**, 1272–1276 (2017).
40. M. Gebhardt, C. Gaida, T. Heuermann, F. Stutzki, C. Jauregui, J. Antonio-Lopez, A. Schulzgen, R. Amezcua-Correa, J. Limpert, and A. Tünnermann, "Nonlinear pulse compression to 43 W GW-class few-cycle pulses at 2 μm wavelength," Opt. Lett. **42**, 4179–4182 (2017).
41. P. Jaworski, F. Yu, R. R. J. Maier, W. J. Wadsworth, J. C. Knight, J. D. Shephard, and D. P. Hand, "Picosecond and nanosecond pulse delivery through a hollow-core negative-curvature fiber for micro machining applications," Opt. Express **21**, 22742–22753 (2013).